



HAL
open science

Resonance Effect Reduction with Bandpass Negative Group Delay Function

Blaise Ravelo, Yajian Gan, Fayu Wan, Wenceslas Rahajandraibe, Sébastien Lalléchère, Zhifei Xu

► **To cite this version:**

Blaise Ravelo, Yajian Gan, Fayu Wan, Wenceslas Rahajandraibe, Sébastien Lalléchère, et al.. Resonance Effect Reduction with Bandpass Negative Group Delay Function. *IEEE Transactions on Circuits and Systems II: Express Briefs*, 2021, 68 (7), pp.2364-2368. 10.1109/TCSII.2021.3059813 . hal-03606636

HAL Id: hal-03606636

<https://hal.science/hal-03606636>

Submitted on 11 Mar 2022

HAL is a multi-disciplinary open access archive for the deposit and dissemination of scientific research documents, whether they are published or not. The documents may come from teaching and research institutions in France or abroad, or from public or private research centers.

L'archive ouverte pluridisciplinaire **HAL**, est destinée au dépôt et à la diffusion de documents scientifiques de niveau recherche, publiés ou non, émanant des établissements d'enseignement et de recherche français ou étrangers, des laboratoires publics ou privés.

Resonance Effect Reduction with Bandpass Negative Group Delay Function

Blaise Ravelo, *Member, IEEE*, Yajian Gan, Fayu Wan, *Member, IEEE*, Wenceslas Rahajandraibe, *Member, IEEE*, Sébastien Lalléchère, *Member, IEEE*, and Zhifei Xu, *Member, IEEE*

Abstract—This paper introduces an original reduction method of resonance effect dispersion by using bandpass negative group delay (NGD) function. The resonance dispersion transfer function (TF) model is parametrized by lumped RLC circuit. The canonical parameters of NGD passive cell are originally formulated as a function of the resonance dispersion specifications. The NGD resonance method feasibility is validated with commercial tool frequency domain simulations. Proof-of-concept circuits constituted by passive RLC-resonant and NGD passive ones are considered. The results confirm an obvious reduction of peak resonance magnitudes and GDs from (18-dB, 10-ns) to better than (2-dB, 2-ns) are realized in the NGD bandwidth of about 80 MHz. The NGD method robustness is also investigated with simultaneous and individual relative variations of the dispersion parameters.

Index Terms—Correction method, Bandpass negative group delay (NGD), Concave dispersion, Synthesis relation.

I. INTRODUCTION

DESPITE the tremendous technological progress, the communication system performance suffers naturally of undesirable delay and resonance perturbations [1-6]. In fact, the degradations of transmission signal are intimately linked to the channel dispersion effect. Several constraints constitute physical factors limiting the electronic system performances. For example, the non-flat transmission gain and the propagation delay related to dispersive channels [6-7] are major one challenging constraints of the communication system design. In addition, the time-varying propagation channel effects degrade considerably the performances of wireless network systems [8]. Some of recent wireless systems were designed with multiagent concept and operating with varying time delays [9].

To face up to this issue of resonance and dispersion effects, an innovative method compared to the complex signal processing approaches is necessary. The present paper is focused on alternative correction method based on the bandpass negative group delay (NGD) function. The NGD equalization

[10] was used and implemented with electronic circuits to neutralize group delay (GD) susceptible to be generated by electrical interconnection RC- and LC-circuit model.

In difference to most of the existing signal correction techniques against the channel dispersive degradation, the NGD method under investigation is implemented in both circuit and system approaches. The analytical implementation can be realized in both the frequency and time domains. Moreover, the NGD method presents an outstanding simplicity and flexibility to any dispersion frequency band. Before exploring the dispersion reduction method, it is worth slightly describing the unfamiliar NGD functions. It is noteworthy that the non-conventional NGD functions behave with mathematical analogy with the classical linear filter gain [11]. Different categories of NGD functions as low-pass, high-pass and bandpass (BP) NGDs were classified. The corrector developed in this paper is originally based on the bandpass NGD function. This particular function attracted recently attention of radiofrequency (RF) and microwave engineers by designing different topologies of bandpass NGD circuits [12-16]. Compact circuit and absorptive filter-based BP NGD circuits were designed [13-14]. The unfamiliar BP NGD function was also implemented with microwave signal interference effects [15-16]. Knowing the “V”-shape behavior [11] regularly associated to the BP NGD magnitude, an original method enabling to reduce the resonance dispersion effect is developed in the paper.

This paper is organized in three main sections, complementary to this introductory part. Based on transfer function (TF) approach, Section II develops the analytical principle of the NGD method under study. The mechanism of the resonance dispersion reduction will be elaborated with mathematical equations including the NGD parameter formulation in function of the dispersion specifications. Section III is focused on the feasibility analysis. Proof-of-concept (POC) circuit will be analyzed with illustrative comparison of

Manuscript received xxx xx, 2020; revised xxx xx, 2020; accepted xxx xx, 2020. Date of publication xxx xx, 2020.

This research work was supported in part by NSFC under Grant 61601233 and Grant 61971230, in part by the Electrostatic Research Foundation of Liu Shanghe Academicians and Experts Workstation, Beijing Orient Institute of Measurement and Test under Grant BOIMTLSHJD20181003, , in part by the Jiangsu Innovation and Enterprise Group Talents Plan 2015 under Grant SRCB201526, and in part by The Priority Academic Program Development of Jiangsu Higher Education Institutions.

Blaise Ravelo and Fayu Wan are with School of Electronic & Information Engineering, Nanjing University of Information Science & Technology

(NUIST), Nanjing, Jiangsu 210044, China (e-mail: blaise.ravelo@nuist.edu.cn, Corresponding author e-mail: fayu.wan@nuist.edu.cn).

Yajian Gan and Wenceslas Rahajandraibe are with the Aix-Marseille University, CNRS, University of Toulon, IM2NP UMR7334, Marseille, France (E-mail: yajian.gan@im2np.fr, wenceslas.rahajandraibe@im2np.fr).

Sébastien Lalléchère is with the Université Clermont Auvergne (UCA), CNRS, SIGMA Clermont, Institut Pascal, Aubière, France. (email: sebastien.lallechere@uca.fr).

Zhifei Xu is with EMC Laboratory, Missouri University of Science and Technology, Rolla, MO 65401, USA. (email: zxfdc@mst.edu).

calculated and simulated magnitudes and GDs of dispersion and NGD TFs. Last, Section IV is the conclusion.

II. THEORY ON THE BANDPASS NGD METHOD OF RESONANCE DISPERSION REDUCTION

This section describes the circuit theory on the dispersion effect reduction. After the canonical definitions of the dispersion, the equivalent passive RLC circuit will be considered. Then, the design formulas of appropriated BP NGD circuit in function of the dispersion parameters will be originally established.

A. Specifications of Resonance Effect

The resonance effect under study is generated by the circuit constituted by R_d , L_d and C_d passive components depicted in Fig. 1(a). By taking $V_1(j\omega)$ and $V_2(j\omega)$ the spectrums of signals referred as ports ① and ②, respectively, the circuit voltage TF can be expressed as:

$$T_d(j\omega) = V_2(j\omega) / V_1(j\omega) = 1 / (L_d C_d s^2 + R_d C_d s + 1) \quad (1)$$

with $s=j\omega=j2\pi f$ the Laplace variable with magnitude $T_d(\omega)=|T_d(j\omega)|$ and phase $\varphi_d(\omega)=\arg[T_d(j\omega)]$. The associated GD is analytically defined by:

$$\tau_d(\omega) = \frac{-\partial\varphi_d(\omega)}{\partial\omega} = \frac{R_d C_d (1 + L_d C_d \omega^2)}{1 + C_d (R_d^2 C_d - 2L_d) \omega^2 + L_d^2 C_d^2 \omega^4}. \quad (2)$$

The dispersion due to the resonance phenomenon can be represented by the TF magnitude and GD responses depicted in Figs. 1(b) and 1(c). The resonance is specified by the center frequency:

$$\omega_0 = \sqrt{2L_d - R_d^2 C_d} / (\sqrt{2}L_d C_d^{1/2}). \quad (3)$$

It can be found that the resonance frequency exists under the condition:

$$L_d > R_d^2 C_d / 2. \quad (4)$$

At ω_0 , the TF presents the magnitude and GD, respectively:

$$T_0 = T_d(\omega_0) = 4L_d^2 / |R_d^2 C_d (4L_d - R_d^2 C_d)|. \quad (5)$$

$$\tau_0 = \tau_d(\omega_0) = 2L_d / R_d. \quad (6)$$

The dispersion effect associated to the resonance is also characterized by the magnitude:

$$T_d(\omega_0 + \Delta\omega/2) = 1 \quad (7)$$

which corresponds to the bandwidth:

$$\Delta\omega = (\sqrt{2} - 1)\omega_0. \quad (8)$$

The associated GD is defined, respectively, by:

$$\tau_d(\omega_0 - \Delta\omega/2) = \tau_0 - \Delta\tau. \quad (9)$$

The resonance dispersion TF can be rewritten in the canonical form:

$$T_d(s) = \omega_0^2 / (s^2 + \zeta\omega_0 s + \omega_0^2) \quad (10)$$

specified by the real parameters:

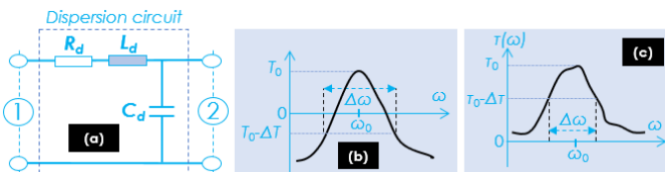


Fig. 1. Dispersion (a) circuit, and TF (b) magnitude and (c) GD specifications.

$$\omega_0 = 1 / \sqrt{L_d C_d} \quad (11)$$

$$\zeta = R_d \sqrt{C_d} / \sqrt{L_d} \quad (12)$$

It can be originally demonstrated that knowing, the peak, T_0 , the resonance TF GD at ω_0 , is expressed as:

$$\tau_0 = \sqrt{2\sqrt{T_0^2 - 1}(T_0 + \sqrt{T_0^2 - 1})} / \omega_0 \quad (13)$$

for any given resonance effect specified at frequency ω_0 , the L_d and C_d parameters can be synthesized by the equations:

$$L_d = R_d \sqrt{\sqrt{T_0^2 - 1}(T_0 + \sqrt{T_0^2 - 1})} / (\sqrt{2}\omega_0) \quad (14)$$

$$C_d = \sqrt{2} / \left[R_d \omega_0 \sqrt{\sqrt{T_0^2 - 1}(T_0 + \sqrt{T_0^2 - 1})} \right]. \quad (15)$$

B. Identification of Appropriated Bandpass NGD Function

To reduce the resonance effect, we will employ the BP NGD function with properties and specifications introduced in this subsection. The bandpass NGD function [16] allows to operate in the signal frequency band where the GD presents a negative value. The NGD function is implemented with the passive cell composed of RLC-parallel network combined to resistance, R_0 as shown in Fig. 2(a). The bandpass NGD function is specified, inversely to the resonance responses of Figs. 1(b) and 1(c), with magnitude and GD responses depicted in Figs. 2(b) and 2(c), respectively. The bandpass NGD function is defined by its NGD center frequency, ω_n , and bandwidth, $\Delta\omega$. The BP NGD voltage TF canonical form can be written as:

$$T_n(s) = T_{n_0} (s^2 + \omega_a s + \omega_n^2) / (s^2 + \omega_b s + \omega_n^2) \quad (16)$$

where:

$$\omega_n = 1 / \sqrt{LC} \quad (17)$$

$$\omega_a = 1 / (RC) \quad (18)$$

$$\omega_b = (R + R_0) / (R_0 RC) \quad (19)$$

At ω_0 , the associated magnitude and GD, which is defined by:

$$\tau_n(\omega) = -\partial \arg[T_n(j\omega)] / \partial\omega \quad (20)$$

are expressed as, respectively:

$$T_n(\omega_0) = |T_n(j\omega_0)| = T_{n_0} \omega_a / \omega_b = R_0 / (R + R_0) \quad (21)$$

$$\tau_n(\omega_0) = 2(\omega_a - \omega_b) / (\omega_a \omega_b) = -2R^2 / [L\omega_0^2 (R + R_0)]. \quad (22)$$

This last expression, $\tau_n(\omega_n) < 0$, is always negative for any value of RLC circuit parameters. This remark confirms the passive cell introduced in Fig. 2(a) behaves as BP NGD function. This linear system can be originally characterized by NGD cut-off frequencies written as:

$$\omega_1 = \omega_n \left[x - L\omega_n (R + R_0) \sqrt{x} \right]^{1/2} / (R\sqrt{R_0}) \quad (23)$$

$$\omega_2 = \omega_n \left[x + L\omega_n (R + R_0) \sqrt{x} \right]^{1/2} / (R\sqrt{R_0}) \quad (24)$$

with:

$$x = L\omega_n^2 (R + R_0) + 2R^2 R_0. \quad (25)$$

C. NGD Function Parameters Analytical Determination

To reduce the resonance effect illustrated in Figs. 1(b) and 1(c), the association of dispersion and BP NGD TFs seems to be an intuitive solution. The following paragraphs describe the analytical mechanism of the NGD function synthesis.

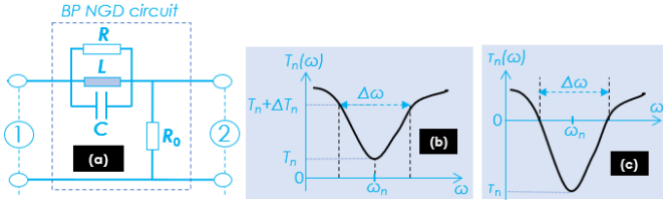


Fig. 2. BP NGD (a) cell and TF (b) magnitude, and (c) GD specified responses.

The design feasibility of the canonical system introduced in (16) is confirmed by these NGD specifications.

1) Principle of Resonance Reduction

To realize the resonance effect reduction, the total TF magnitude and GD are expected to behave as presented in Fig. 3(a) and Fig. 3(b). It means that the associated TF must be close to unity $T(s) \approx 1$. Because of dispersion, the output of system introduced in Fig. 1(b-c) is distorted compared to input, $V_2 \neq V_1$. To overcome this undesirable dispersion issue, the aim of correction consists in introducing a solution allowing to generate corrected output $V_2 = T(V_1) \approx V_1$ especially, in the frequency band $[\omega_0, \Delta\omega]$. The developed resonance reduction principle is aimed to introduce the BP NGD function. The correction technique under investigation consists originally in cascading the resonance and NGD circuits as illustrated in Fig. 3(c). Under the consideration of the inter-stage matching follower, the total circuit TF can be analytically modelled by:

$$T(s) = T_d(s) \times T_n(s). \quad (26)$$

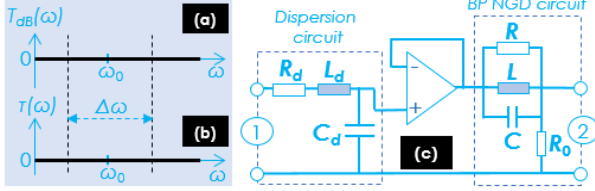


Fig. 3. Desired TF (a) magnitude and (b) GD specifications of (c) cascaded dispersion-NGD circuit.

2) NGD Parameters Synthesis Formulation in Function of Resonance Specifications

This paragraph describes the analytical mechanism of the dispersion correction NGD method. As target of the analysis, the NGD TF parameters must be determined in function of the resonance parameters introduced in Figs. 1. The resonance effect reduction means the annihilation of the total TF proposed in equation (26). In other words, by taking $\omega_n = \omega_0$, the corrected dispersion TF magnitude and GD must be close to:

$$T(\omega_0) = T_d(\omega_0) \times T_n(\omega_0) \approx 1 \quad (27)$$

$$\tau(\omega_0) = \tau_d(\omega_0) + \tau_n(\omega_0) \approx 0. \quad (28)$$

Knowing the dispersion and NGD transmittances defined in equation (10) and equation (16), the dispersion effect reduction can be realized by synthesizing the NGD circuit parameters R , L and C knowing T_0 , ω_0 and for the given resistance load, R_0 . It yields from equation (27), the inversion of equation $T_{n0} = 1/T_0$, and equation (21), the NGD parameter synthesis relation:

$$R = (T_0 - 1)R_0. \quad (29)$$

It can be derived from equation (28) and the GD expressed in equation (22), the dispersion GD annihilation leads to the inductance synthesis equation:

$$L = \sqrt{2}R_0(T_0 - 1)^2 / \left\{ \omega_0 \left[T_0 (T_0^2 - 1)^{1/2} + T_0^2 - 1 \right]^{1/2} \right\}. \quad (30)$$

By inversion of resonance frequency, $\omega_n = \omega_0$, of equation (17), we have the capacitor formula:

$$C = T_0 \left[T_0 (T_0^2 - 1)^{1/2} + T_0^2 - 1 \right]^{1/2} / \left[\sqrt{2}R_0\omega_0(T_0 - 1)^2 \right]. \quad (31)$$

III. PROOF-OF-CONCEPT OF RESONANCE EFFECT REDUCTION WITH BP NGD CIRCUIT

The present section deals with the validation of the previous theoretical approach. A POC constituted by a lumped circuit generating the resonance effect reduction and corrected with a BP NGD function will be investigated based on the frequency domain or AC analyses. This validation study consists mainly in comparing the responses from the dispersion, NGD and both combined NGD-dispersions TFs expressed in (1), (16) and (27), respectively, calculated with Matlab and simulations.

A. Validation with POC Simulated Results

The dispersion parameters (T_0, f_0) were arbitrarily chosen to validate the NGD resonance effect reduction. The associated RLC resonant circuit inductance, L_d and capacitance, C_d , addressed in Table I, were calculated from equations (14) and (15) by fixing the value of resistor, $R_d = 10 \Omega$. As previously mentioned, these values were assumed for the purpose of illustration. Depending on the given application, the ranges listed in Table I may be freely adapted (see e.g. in [6] when focusing on resonances). The BP NGD function parameters, R , L and C were synthesized by mean of formulas (29), (30) and (31) by assuming $R_0 = 50 \Omega$. The POC dispersion-NGD circuit simulated in the schematic environment of the ADS® commercial tool from Keysight Technologies® is displayed in Fig. 4(a). A follower is inserted between the two circuit blocks for the inter-stage matching. The AC analysis was carried in the frequency band delimited from 0.15 GHz to 0.35 GHz. The significant flatness of magnitudes and GDs of TF, respectively displayed in Figs. 4(b) and 4(c), reveals the effectiveness of the NGD resonance reduction method.

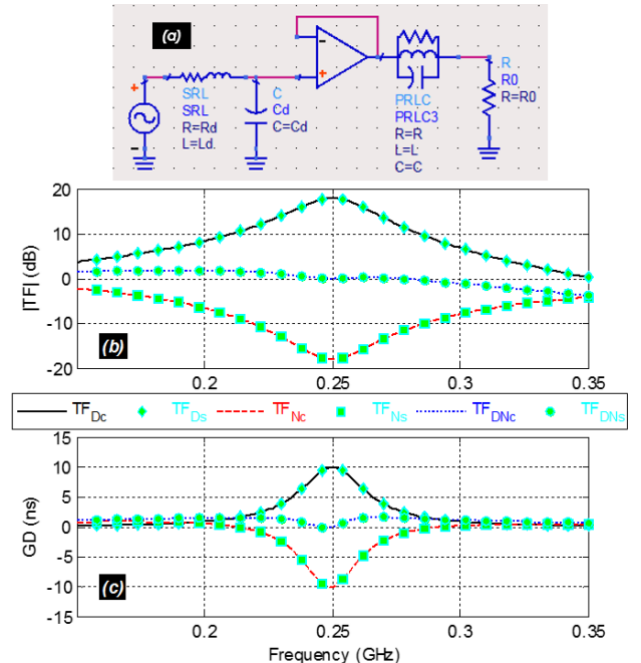


Fig. 4. (a) POC circuit. Comparisons of calculated (solid line) and simulated (dotted line) TF (b) magnitude and (c) GD responses.

TABLE I

POC DISPERSION AND NGD CIRCUIT PARAMETERS, AND SPECIFICATIONS

Dispersion Specification	Parameter	f_0	T_0	τ_0
	Value	0.25 GHz	18 dB	10 ns
	Parameter	R_d	L_d	C_d
Value	10 Ω	50 nH	8 pF	

NGD	Parameter	R_d	L_d	C_d
	Value	10 Ω	50 nH	8 pF
	Parameter	$T_n(f_0)$	τ_0	f_1
Value	-17.95 dB	-10 ns	213 MHz	293 MHz

Dispersion-NGD	Parameters	$T(f_0)$	$GD(f_0)$
	Value		1.91 dB

The calculated (“ TF_{Dc} ,” “ TF_{Nc} ” and “ TF_{DNc} ”) and simulated (“ TF_{Ds} ,” “ TF_{Ns} ” and “ TF_{DNs} ”) responses, plotted in solid and dotted curves, respectively are in excellent agreement. The dispersion, NGD and total TF responses, denoted TF_D , TF_N and TF_{DN} , respectively are plotted in solid black, red dashed and blue dotted curves, respectively. Table I summarizes the magnitude and GD values around the considered center frequency, f_0 . Thanks to the BP NGD function with cut-off frequencies, $\omega_{1,2} = 2\pi f_{1,2}$ (expressed in equations (23) and (24)), under 80 MHz NGD bandwidth, an obvious reduction of resonance magnitude TF_D is observed compared to TF_{DN} , and also the GD GD_{TFD} compared to GD_{TFDN} in the NGD frequency band. As expected, the total TF TF_{DN} of dispersion-NGD circuit presents a better flatness with value much closer to 0 dB (or unity TF).

B. Parametric Analyses with Respect to R_d , L_d and C_d

To demonstrate the NGD method robustness, AC analyses with respect to the dispersion variables (R_d, L_d, C_d) assumed fluctuating between $\pm 5\%$ were investigated. For this parametric analyses, five different test cases were considered as seen in Table II. The resonance frequency decreases from 264 to 239 MHz. The suitable parameters (R, L, C) of NGD circuit were calculated in function of variables (R_d, L_d, C_d) via formulas (29), (30) and (31) with $R_0 = 50 \Omega$ and $GD(f_0) = -10$ ns. As results, we obtain the performances of the dispersion-NGD corrected circuit indicated in Table II. The dispersion, NGD and dispersion-NGD circuit responses are plotted in dashed, dotted and solid curves shown in Figs. 5. As expected, excellent corrections of resonance dispersion effect are performed for each cases of variables (R_d, L_d, C_d). Total TF close to unity is realized with the peaks of magnitude reduced from 18.5 dB to 2 dB and GD from 10 ns to 1.83 ns.

C. Parametric Analyses with Individual Variations of Dispersion Circuit Parameters, R_d , L_d and C_d

The effectiveness of the developed NGD method with the individual variations of R_d , L_d and C_d is investigated in the present subsection. In difference to the study presented in the previous subsection, in this part, we assume that the same NGD circuit with the initial parameters calculated in Table I. Then, the AC analyses of dispersion, NGD and dispersion-NGD circuits were performed. The results of each dispersion parameter effects are highlighted by the magnitude and GD responses given in Figs. 6. For the purpose of the illustration, it is to be noted the parametric analysis is achieved varying each of the three parasitic terms R_d , L_d and C_d , with respect with the constitutive relations (14) and (15).

Moreover, the NGD method performances with the variations

TABLE II

 R_d, L_d AND C_d SIMULTANEOUS VARIATION DISPERSION REDUCTION RESULTS

Case	1	2	3	4	5	
Dispersion	R_d (Ω)	9.5	9.75	10	10.25	10.5
	L_d (nH)	47.5	48.75	50	51.25	52.5
	C_d (pF)	7.64	7.84	8.04	8.24	8.44
	f_0 (MHz)	264	257	251	245	239
	T_0 (dB)	18.4	18.17	17.95	17.74	17.53
NGD	τ_0 (ns)	10	9.99	10	10	10
	R (Ω)	365.8	355.2	345.1	335.5	326.3
	L (nH)	23.35	23.8	24.23	24.66	25.09
	C (pF)	15.54	16.06	16.59	17.12	17.67
	f_1 (MHz)	226	220	214	209	204
D_N	f_2 (MHz)	308	301	294	287	280
	$T(f_0)$ (dB)	1.98	2	2.02	2.04	2.06
	$GD(f_0)$ (ns)	1.63	1.68	1.73	1.78	1.83

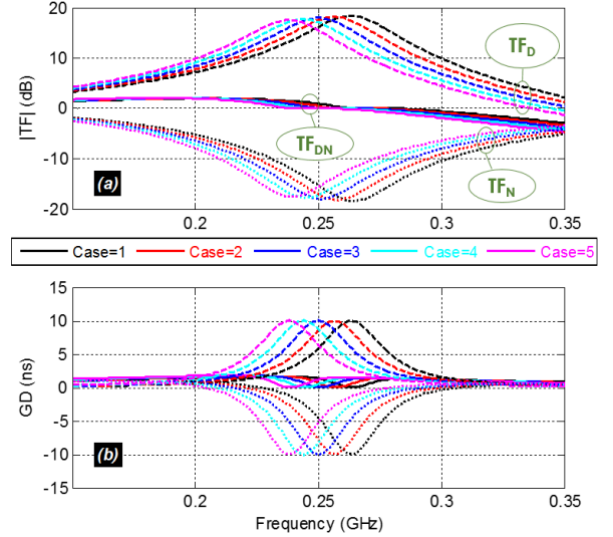


Fig. 5. TF (a) magnitudes and (b) GDs of dispersion (TF_D), NGD (TF_N) and both combined (TF_{DN}) circuits for the different cases indicated in Table II.

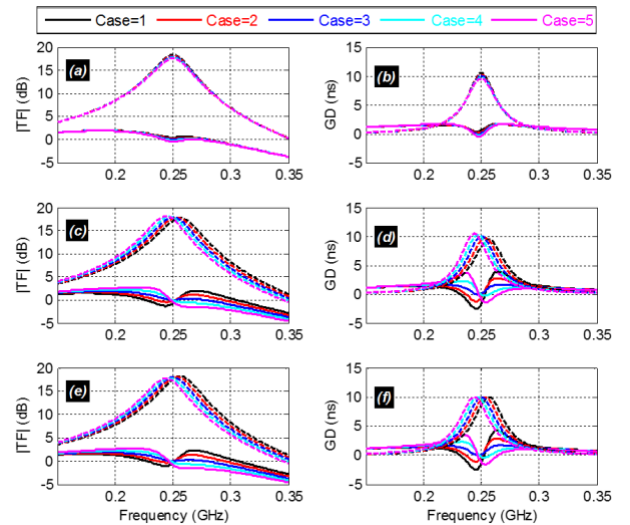


Fig. 6. TF magnitudes and GDs of dispersion (dashed lines) and both NGD-dispersion circuits (plain lines) for the different cases indicated in Table III under (a-b) R_d , (c-d) L_d and (e-f) C_d variations.

of R_d , L_d and C_d can be quantified with the magnitudes and GDs summarized in Tables III, IV and V, respectively. The magnitude and GD responses are shown in:

- Figs. 6(a) and 6(b) for the R_d $\pm 5\%$ variation by fixing L_d and C_d . It can be seen that this resistive variation does not

affect significantly the dispersion responses. However, the NGD influence is obviously confirmed by the solid curves with reduction of magnitude and GD peaks around f_0 . From 18.4 dB to 1.93 dB, and 10.5 ns to 1.7 ns.

- Figs. 6(c) and 6(d) for the $L_d/\pm 5\%$ variation by fixing R_d and C_d . As expected, it is to be noted that this inductive effect variation affects principally the resonance frequency and the peaks of both magnitude and GD. As illustrated by Fig. 6(c), the NGD influence is confirmed by the decrease of the magnitude from 18.16 dB to 2.72 dB. Then, the GD is decreased from 10.51 ns to 3.67 ns. The degraded quality of NGD-dispersion responses is due to the mismatch between the dispersion resonance frequency f_0 and the BP NGD centre frequency.
- Figs. 6(e) and 6(f) highlight the influence of the $C_d/\pm 5\%$ variation by fixing R_d and L_d . In this configuration, both the resonance frequency and magnitude are changing significantly. Then, the BP NGD function reduce again the resonance effect with reduction from 17.74 dB to 2.63 dB, and the GD from 10 ns to 3.47 ns. Similar to the previous configuration, the mismatch between the dispersion resonance and NGD centre frequency explains the less significant effectiveness of the method.

TABLE III
DISPERSION REDUCTION RESULTS WITH R_d VARIATIONS

Case	1	2	3	4	5
R_d (Ω)	9.5	9.75	10	10.25	10.5
L_d (nH)	50				
C_d (pF)	8				
f_0 (MHz)	250				
T_0 (dB)	18.4	18.17	17.95	17.74	17.53
τ_0 (ns)	10.53	10.26	10	9.76	9.53
$T(f_0)$ (dB)	1.93	1.92	1.91	1.9	1.89
$GD(f_0)$ (ns)	1.7	1.69	1.69	1.69	1.7

TABLE IV
DISPERSION REDUCTION RESULTS WITH L_d VARIATIONS

Case	1	2	3	4	5
R_d (Ω)	10				
L_d (nH)	47.5	48.75	50	51.25	52.5
C_d (pF)	8				
f_0 (MHz)	263	257	250	244	238
T_0 (dB)	17.73	17.84	17.95	18.06	18.16
τ_0 (ns)	9.5	9.76	10	10.25	10.51
$T(f_0)$ (dB)	2.03	1.66	1.91	2.22	2.72
$GD(f_0)$ (ns)	3.93	2.79	1.69	2.31	3.67

TABLE V
DISPERSION REDUCTION RESULTS WITH C_d VARIATIONS

Case	1	2	3	4	5
R_d (Ω)	10				
L_d (nH)	50				
C_d (pH)	7.64	7.84	8.04	8.24	8.44
f_0 (MHz)	263	220	214	209	204
T_0 (dB)	18.17	18.06	17.95	17.85	17.74
τ_0 (ns)	10				
$T(f_0)$ (dB)	2.33	1.67	1.91	2.2	2.63
$GD(f_0)$ (ns)	4.21	2.88	1.69	2.3	3.47

IV. CONCLUSION

An original reduction of resonance dispersion effect by using BP NGD function is initiated. The mechanism of the outstanding simple and efficient NGD method is described with TF approach. The design equations of appropriated BP NGD circuit in function of the dispersion parameters are formulated. The NGD method feasibility is illustrated with frequency

domain analyses by considering passive RLC circuits. Calculated and simulated results are in excellent agreement; the outstanding TF flatness improvement confirms the effectiveness of the NGD method. Parametric analyses in function of the resonance dispersion variables are carried out to illustrate the method robustness.

Applicative study with demonstrators is under the prospect of this study. As ongoing research, an application of the BP NGD correction to wireless multipath channel dispersion is currently in progress.

REFERENCES

- [1] M-E. Hwang, S-O. Jung and K. Roy, "Slope Interconnect Effort: Gate-Interconnect Interdependent Delay Modeling for Early CMOS Circuit Simulation," IEEE Trans. CAS I, Vol. 56, No. 7, Jul. 2009, pp. 1428-1441.
- [2] G. Groenewold, "Noise and Group Delay in Active Filters," IEEE Trans. CAS I: Regular Papers, Vol. 54, No. 7, July 2007, pp. 1471-1480.
- [3] C. Wijenayake, Yongsheng Xu, A. Madanayake, L. Belostotski and L. T. Bruton, "RF Analog Beamforming Fan Filters Using CMOS All-Pass Time Delay Approximations," IEEE Trans. CAS I: Regular Papers, Vol. 59, No. 5, May 2012, pp. 1061-1073.
- [4] K. J. Kim, M. D. Renzo, H. Liu, P. V. Orlik and H. V. Poor, "Performance Analysis of Distributed Single Carrier Systems With Distributed Cyclic Delay Diversity," IEEE Trans. Comm, vol. 65, no. 12, Dec. 2017, pp. 5514-5528.
- [5] X. Lei, Y. Song, X. Yao, B. Dong and M. Jin, "Effect of Group Delay on Channel Estimation Performance in OFDM System," Appl. Math. Inf. Sci., vol. 6-3S, no. 3, 2012, pp. 1037-1045.
- [6] M. Bertocco, A. Sona, "Analysis and Mitigation of EMC Effects of Electric Resonances in Circuits", in Proc. 2018 Int. Symp. On EMC, EMC Europe 2018, Amsterdam, The Netherlands, Aug. 2018
- [7] Z. Zhang and C. L. Law, "Short-Delay Multipath Mitigation Technique Based on Virtual Multipath," IEEE Ant. Wireless Propag. Lett., Vol. 4, 2005, pp. 344-348.
- [8] T. Li, W.-A. Zhang and L. Yu, "Improved Switched System Approach to Networked Control Systems With Time-Varying Delays," IEEE Trans. Control Systems Technology, vol. 27, no. 6, Nov. 2019, pp. 2711-2717.
- [9] Q. Xiong, P. Lin, W. Ren, C. Yang and W. Gui, "Containment Control for Discrete-Time Multiagent Systems With Communication Delays and Switching Topologies," IEEE Trans. Cybernetics, vol. 49, no. 10, Oct. 2019, pp. 3827-3830.
- [10] B. Ravelo, "Neutralization of LC- and RC-Effects with Left-Handed and NGD Circuits," Advanced Electromagnetics (AEM), vol. 2, no. 1, Sept. 2013, pp. 73-84.
- [11] B. Ravelo, "Similitude between the NGD function and filter gain behaviours," Int. J. Circ. Theor. Appl., vol. 42, no. 10, Oct. 2014, pp. 1016-1032.
- [12] G. Liu and J. Xu, "Compact transmission-type negative group delay circuit with low attenuation," Electron. Lett., vol. 53, no. 7, pp. 476-478, Mar. 2017.
- [13] T. Shao, Z. Wang, S. Fang, H. Liu, and S. Fu, "A compact transmission line self-matched negative group delay microwave circuit," IEEE Access, vol. 5, pp. 22836-22843, Oct. 2017.
- [14] L.-F. Qiu, L.-S. Wu, W.-Y. Yin, and J.-F. Mao, "Absorptive bandstop filter with prescribed negative group delay and bandwidth," IEEE Microw. Wireless Compon. Lett., vol. 27, no. 7, pp. 639-641, Jul. 2017.
- [15] Z. Wang, Y. Cao, T. Shao, S. Fang and Y. Liu, "A Negative Group Delay Microwave Circuit Based on Signal Interference Techniques," IEEE Microw. Wireless Compon. Lett., vol. 28, no. 4, pp. 290-292, Apr. 2018.
- [16] F. Wan, N. Li and B. Ravelo, "O=O Shape Low-Loss Negative Group Delay Microstrip Circuit," IEEE Trans. CAS II: Express Briefs, Early Access, 2019, pp. 1-5

